Published in final edited form as:
Birth Defects Res A Clin Mol Teratol. 2013 June ; 97(6): 373–385. doi:10.1002/bdra.23149.

Periostin Downregulation Is an Early Marker of Inhibited Neonatal Murine Lung Alveolar Septation

Shawn K. Ahlfeld[*], **Yong Gao**, **Jian Wang**, **Emrin Horgusluoglu**, **Esther Bolanis**, **D. Wade Clapp**, and **Simon J. Conway**[*]
Developmental Biology and Neonatal Medicine Program, HB Wells Center for Pediatric Research, Indiana University School of Medicine, Indianapolis, Indiana

Abstract

BACKGROUND—Extreme preterm birth exposes the saccular lung to multiple teratogens, which ultimately retard alveolar development. Specifically, therapeutic high level oxygen supplementation adversely affects the premature lungs and results in blunted alveolarization. Prolonged hyperoxic lung injury has previously been shown to upregulate the matricellular protein Periostin (Postn) and stimulate ectopic accumulation of alpha smooth muscle actin (αSMA) myofibroblasts. Therapies that promote lung septation are lacking largely due to a lack of reliable early biomarkers of injury. Thus, we determined if Postn expression correlated with the initial appearance of myofibroblasts in the saccular lung and was required for early alveolar development.

METHODS—Lung development in C57BL/6J mice following room-air (RA, 21%-O_2) or continu ous hyperoxia (85%-O_2) from birth (P0) through postnatal day P14 was correlated with Postn and αSMA expression. Alveolarization in *Postn* knockout mice exposed to room-air, 60%-, and 85%-O_2 was also examined.

RESULTS—Postn was widely expressed in distal lung septa through P2 to P4 and peak expression coincided with accumulation of saccular myofibroblasts. Initially, 85%-O_2 prematurely downregulated Postn and αSMA expression and suppressed proliferation before the first evidence of distal lung simplification at P4. By P14, chronic 85%-O_2 resulted in secondary upregulation of Postn and αSMA in blunted septa. Myofibroblast differentiation and alveolar development was unaffected in *Postn* null mice and acute 85%-O_2 exposure equally inhibited septal formation in *Postn* null and wild-type littermates.

CONCLUSION—Postn expression is tightly correlated with the presence of αSMA-myofibroblasts and is a novel early biomarker of acutely inhibited alveolar septation during a crucial window of lung development.

Keywords

neonatal lung morphogenesis; bronchopulmonary dysplasia; hyperoxia; Postn; alpha smooth muscle actin; myofibroblast

[*]Correspondence to: Simon J. Conway or Shawn K. Ahlfeld, 1044 West Walnut Street, Room R4 W402E, Indiana University School of Medicine, Indianapolis, IN 46202. siconway@iupui.edu and skahlfel@iu.edu.

INTRODUCTION

Infants at term gestation are born with mature saccular lungs which are primed to undergo rapid postnatal alveolarization. During alveolarization, myofibroblasts expressing alpha smooth muscle actin (αSMA) secrete elastin, collagen, and other extracellular matrix components propel the growth of secondary septa from the mature saccular wall during the first 6 to 24 months of life (Roth-Kleiner et al., 2004; Burri, 2006). The result is a vastly increased surface area for gas exchange. Thus, optimal postnatal distal lung complexity depends on complex molecular networks which are initiated in utero to establish and orchestrate timely remodeling of lung structure (Morrisey and Hogan, 2009). The preparations for postnatal alveolarization occur during canalicular and saccular lung development and are designed to occur in a sterile, fluid-filled, relatively hypoxic in utero environment. Advances in neonatal care have allowed for the survival of extremely preterm infants before 28 weeks gestation (Stoll et al., 2010), and, therefore, the premature developing saccular lung is routinely exposed to an abnormal environment. Multiple teratogens (defined as any agent that can disrupt normal development) associated with preterm birth including preeclampsia and chorioamnionitis, as well as life-sustaining interventions like mechanical ventilation and excessive supplemental oxygen, can disrupt the complex molecular pathways required for normal saccular and early alveolar lung development (Van Marter, 2009; Ahlfeld and Conway, 2012). As a result, the majority of extremely preterm infants develop bronchopulmonary dysplasia (BPD), a chronic lung birth defect characterized by simplified distal airspaces and diagnosed clinically by the need for supplemental oxygen (Husain et al., 1998; Coalson, 2006). Moreover, BPD results in long-lasting deficits of lung function (Vrijlandt et al., 2006; Baraldi et al., 2009; Balinotti et al., 2010; Fawke et al., 2010).

The matricellular protein, Periostin (Postn), has recently been associated with excessive myofibroblast accumulation resulting in fibrotic lung disease and alveolar simplification in neonatal mice exposed to hyperoxia throughout saccular and alveolar development (Bozyk et al., 2012). In the same report, upregulation of Postn was observed in lungs of preterm infants that had died of severe BPD. While this late upregulation of Postn identifies advanced, severe BPD, the majority of infants survive with mild-to-moderate forms of the disease (Stoll et al., 2010) and, by definition, all infants with BPD display significantly inhibited alveolarization well before the stage of lung development represented at 14 days in mice (Kimura and Deutsch, 2007). Additionally, the presence of myofibroblasts in the saccular lung is required for early alveolar septation (Lindahl et al., 1997; Boström et al., 2002; Lau et al., 2011), and expression of Postn is required for fibroblastic differentiation during development (Butcher et al., 2007; Snider et al., 2008; Norris et al., 2009). However, Postn expression within these earlier stages has not been examined and it remains unknown if Postn similarly directs myofibroblast differentiation required for normal lung septation. Therefore, the current study was designed to determine if Postn expression was spatiotemporally correlated with normal myofibroblast accumulation in the saccular and early alveolar lung. We also investigated whether changes in Postn expression accompanied early alterations in myofibroblast expression in a physiological hyperoxia murine model of inhibited alveolar septation and whether systemic loss of *Postn* in knockout mice was

sufficient to cause abnormal lung development or whether the systemic loss of *Postn* exacerbated the physiological effects of excessive hyperoxia-induced neonatal lung septation defects. Our results indicate that Postn expression is wide-spread in the distal saccular lung and peak expression coincides with peak expression of αSMA within the saccular wall. Importantly, significant downregulation of Postn precedes inhibited alveolar septation during a window of saccular development capable of persistently nhibiting alveolarization. However, the presence of Postn is not an absolute requirement for normal myofibroblast differentiation, early alveolar septation, or ultimate alveolar complexity. Likewise, the absence of Postn does not preserve alveolar septation in acute hyperoxia. Nevertheless, these data revealed that Postn is a novel, early biomarker of myofibroblast accumulation. Additionally, an acute reduction in Postn during early alveolar septation accompanies inhibited murine septal development and may have utility in identifying early BPD pathogenesis. Given the predominate literature correlating upregulation of Postn with fibrosis and cancer (reviewed in Ruan et al., 2009; Uchida et al., 2012), our report adds to the relative paucity of literature (Yoshioka et al., 2002; Kim et al., 2005) identifying the downregulation of Postn as an equally important marker of disease.

METHODS

Mice Models and Hyperoxia Exposure

Wild-type C57BL/6J (purchased from Jackson Laboratory) and *Postn* knockout mice backcrossed for eight generations onto a C57BL/6J background were used. The generation and genotyping of *Postn* targeted mice, in which the translation start site, all of the first exon, and ~300 bp of the first intron were deleted, was described previously (Rios et al., 2005). For the hyperoxia studies, two or more litters of mice born within 6 hr of one another were pooled and separated into two equal groups of 6 to 8 mice by 12 hr of age. Half of the pups were maintained in a 30″ × 20″ × 20″ polypropylene chamber (BioSpherix, Lacona, NY) in which the oxygen concentration was tightly controlled at 85% O_2 and the other half were maintained in room-air (21% O_2). The choice of 85% hyperoxia was based on previous studies demonstrating the ability to accurately model the inhibition of alveolar development similar to that observed in human infants with BPD (Husain et al., 1998; Warner et al., 1998). Nursing dams were rotated between groups every 48 hr to prevent oxygen toxicity. Oxygen levels were maintained at ± 1% with a Pro-Ox 110 oxygen controller (BioSpherix, Lacona, NY). Humidity and CO_2 levels were maintained within the ambient range of the facility. Pups were continuously exposed until harvested for analysis at postnatal days (P) 2, 4, 7, and 14. A separate cohort of pups were continuously exposed to 85% O_2 from P0 to P4, recovered in room-air, and subsequently harvested for analysis at postnatal day P28. *Postn* knockout mice were killed for analysis at P4 and P7 and compared with age-matched littermate controls for analysis. All procedures were performed with the approval of the Institutional Animal Care and Use Committee of Indiana University School of Medicine (protocol #10107).

Lung Histology and Tissue Processing

Following CO_2 euthanization and aortic transection, the right ventricle was injected with cold PBS until the lungs were visually clear of blood. A tracheotomy was performed and a

22-g syringe adapter inserted and secured with suture. Lungs were inflation-fixed with 4% paraformaldehyde at a constant pressure of 25 cmH_2O for 45 min. The cannula was removed, the suture was tightened to maintain pressure, and the heart and lungs removed en bloc and submerged in 4% paraformaldehyde overnight at 4°C. The entire left lobe of each animal was then dehydrated in a series of graduated ethanols, cleared in xylene, paraffin embedded, and serially sectioned (7 μm thickness) in entirety.

Morphometric Analysis

Serial, equidistant sections through the entire left lung were Hematoxylin/Eosin (H/E) stained and random fields containing distal airspaces were photographed with a 20× objective on a Zeiss Axioskop2Plus Microscope at 1292 × 968 pixels. To assess distal airspace maturation, computer-aided morphometric analysis was performed using ImageJ with a custom plug-in as previously described (Balasubramaniam et al., 2006) to measure mean linear intercept (MLI), nodal density, and septal thickness. For septal thickness, a binary image is formed and seven equidistant horizontal lines are drawn across the field. The length of each line segment that bisects septal tissue is calculated, averaged for the entire field, and reported in micrometers. For analysis, 12 nonoverlapping fields from at least 6 slides per animal were obtained, and at least 3 to 5 animals per condition at each time point were examined. Only fields consisting of alveolar septa were used for analysis; fields containing large vessels, conducting airways, or sectioning artifacts were avoided.

Immunohistochemical Staining

Immunohistochemical staining used the Vectastain Elite ABC kit (Vector Labs, Burlingame, CA) per the manufacturer's directions with diaminobenzidine (DAB, Vector Labs) and hydrogen peroxide as chromogens. The dilution of primary antibodies was 1:18,500 for rabbit anti-Postn (Kruzynska-Frejtag et al., 2004), 1:5000 for rat anti-alpha Smooth muscle actin (αSMA; Sigma), and 1:25 for rat anti-Ki67 (Dako). TUNEL staining was detected in paraffin sections using the In Situ Cell Death Detection kit (Roche). Wild-type littermates were always used as age-matched controls.

In Situ Hybridization

Sense and anti-sense [^{35}S]UTP-radiolabeled *Postn* RNA probes were transcribed for in situ hybridization as described (Conway, 1996). Specific signal was observed only with the anti-sense probe and when detected in at least 3 consecutive sections.

Western Blot Analysis

Lungs were snap frozen in liquid nitrogen and homogenized in ice-cold lysis buffer (0.2 M Tris, 0.01 M EDTA, 0.1 M NaCl and 1% sodium dodecyl sulfate) supplemented with 1 mM sodium orthovanadate, 1 mM sodium fluoride, 100 mM phenylmethanesulfonylfluoride, and a protease inhibitor cocktail (Roche, Indianapolis, IN). Equal amounts of protein (20 μg) were separated by sodium dodecyl sulfate polyacrylamide gel electrophoresis and transferred to a polyvinylidene membrane. Blots were blocked and incubated overnight at 4°C with rabbit anti-Postn (1:5000) (Kruzynska-Frejtag et al., 2004) or mouse anti-αSMA (1:75,000, Sigma). Signal was detected by means of ECL^{Plus} (Amersham) and the

appropriate peroxidase-conjugated secondary antibodies (1:5000). All blots were subsequently stripped (0.2 M NaOH for 5 min at room temperature), thoroughly washed, re-blocked and then probed with mouse anti-α-Tubulin (1:10,000, Sigma). Triplicate X-ray films were scanned and signal intensity measured using ImageJ software (downloaded from wsr@nih.gov) and normalized to α-Tubulin.

Statistical Analysis

Statistical analysis was performed with Prism software (Graphpad Software, San Diego, CA). Comparisons between experimental groups (room-air vs. hyperoxia and null vs. control) were made using unpaired student's *t* test. One-way analysis of variance with Tukey's multiple comparisons test was used to compare Postn and αSMA expression from P0 to P14. A p-value < 0.05 was considered statistically significant. All data are presented as means ± SEM.

RESULTS

αSMA and Postn Expression in the Developing Lung Are Similarly Disturbed during the Early and Late Phases of Continuous Hyperoxia Exposure

Although upregulation of alveolar Postn expression has been implicated in the abnormal accumulation of αSMA^+-myofibroblasts in chronic hyperoxia-induced fibrotic lung disease (Bozyk et al., 2012), it has not been clear whether a similar relationship exists between αSMA^+-myofibroblasts and Postn during the early, acute phase of hyperoxic lung injury during saccular lung development. Thus, we examined the spatiotemporal expression profiles of αSMA protein, a surrogate marker of myofibroblasts (Mitchell et al., 1990; Yamada et al., 2005), and the Postn matricellular protein during the early phase of hyperoxia exposure during saccular and early alveolar lung development (P0–P7) and compared these data with those known for late responses to prolonged hyperoxia into late alveolar development (P14). Significantly, neonates exposed to 85% hyperoxia from birth onward exhibited distal airspace simplification as early as P4 (Fig. 1A,D; Table 1) when compared with age-matched room-air littermate controls. Moreover, hyperoxia-induced blunted airspace phenotype became more apparent at P7 (Table 1). Immunohistochemistry revealed that αSMA-positive myofibroblasts were predominately located around the large airways and major pulmonary vasculature and were beginning to localize within emerging septal tips in P4 room-air control lungs (Fig. 1E). However, in P4 lungs exposed to hyperoxia (Fig. 1B), αSMA-positive myofibroblasts were only detected around the large airways and pulmonary vasculature. Similarly, while Postn was essentially absent from saccular walls in O_2-exposed animals at P4 (Fig. 1C), it was widely expressed throughout septa, including the septal tips, in room-air control lungs (Fig. 1F). Consistent with previous reports (Warner et al., 1998), chronic exposure to continuous hyperoxia arrested secondary septation and resulted in profound alveolar simplification in P14 lungs and a BPD-like phenotype (Fig. 1G; Table 1). Significantly, discrete cellular foci of ectopic αSMA-positive cells abnormally persisted within hyperoxia-exposed simplified alveolar walls at P14 (Fig. 1H), despite the absence of αSMA-positive myofibroblasts from normal alveolar septa (Fig. 1K). Correspondingly, hyperoxia-exposed P14 lungs had a persistence of punctate Postn expression predominantly within the simplified alveolar walls (Fig. 1I), in contrast to normal

room-air P14 lungs in which Postn was strictly confined to the perivascular tissue (Fig. 1L). To quantify these spatial expression changes and verify the bi-phasic misexpression patterns of αSMA and Postn, we used Western blotting of whole P0 to P14 lungs (Fig. 1M). Early on, hyperoxia significantly reduced total lung levels of αSMA at P2 and P4 by 35% and 30%, respectively ($p < 0.05$). Postn protein was also dramatically reduced by 50% at P2 and 60% at P4 ($p < 0.05$) in O_2-exposed lungs. Although there are four Postn isoforms (≈ 90, 87, 85, and 82 kDa) (Snider et al., 2008), only the three largest isoforms are detected in normal neonatal lungs. However, the two largest isoforms are suppressed significantly in both P2 and P4 O_2-exposed lungs (Fig. 1M, 2 top arrows), but the 85kDa isoform is only minimally reduced (Fig. 1M, bottom arrow). However, with continued exposure to hyperoxia through P14, both αSMA and Postn are significantly elevated (68% and 340%, respectively, compared with room-air, $p < 0.05$), consistent with previous reports (Hirakawa et al., 2007; Bozyk et al., 2012; Jiang et al., 2012) and with onset of fibrosis (data not shown). Thus, although both αSMA and Postn are elevated and ectopically located following prolonged hyperoxia, they are initially downregulated significantly within the saccular walls and emerging septal tips coincident with hyperoxia-induced blunted alveolar morphogenesis. To our knowledge, this is the first report of reduced Postn levels in early hyperoxia-induced blunted alveolarization. Moreover, the finding that Postn is downregulated in neonatal lungs as early as P2, establishes Postn as an early ECM marker of hyperoxia-induced pathological lung dysfunction, and provides a novel secreted biomarker of myofibroblast function. Additionally, these results strongly suggest that the altered secretion of Postn in neonatal lungs was a result of the teratogenic effects of elevated O_2 levels.

Postn Is Widely Expressed in the Saccular Lung Coincident with the Accumulation of αSMA$^+$-Myofibroblasts

As Postn appeared to correlate with αSMA expression profiles in normal lungs as well as being co-suppressed by means of hyperoxia, we further examined the spatiotemporal expression of these two ECM proteins during normal early lung septal morphogenesis. Postn is known to promote differentiation of mesenchymal cells into fibroblastic lineages (Butcher et al., 2007; Snider et al., 2008; Norris et al., 2009) and stimulate expression of αSMA (Shimazaki et al., 2008; Jackson-Boeters et al., 2009; Elliott et al., 2012). However, its expression during myofibroblast differentiation in early secondary alveolar septation has not been examined. Given the correlation of Postn and αSMA protein misexpression we observed with both early and late phases of continuous hyperoxia, as well as the downregulation of both proteins preceding the first signs of inhibited secondary septation, we focused our studies to early distal airspace development. Indeed, *Postn* mRNA was absent from distal saccules at P0 but quickly appeared within discrete mesenchymal cells throughout the saccular walls by P2 (Fig. 2A,B). Although still detectable, it was diminished in the alveolar wall by P4 and P7 and absent in P14 lungs (Fig. 2C–E). Similar to mRNA expression, Postn protein was absent from the saccular wall and confined to the large blood vessels at P0 (Fig. 2F). However, by P2 and through P4 Postn was widely expressed; it was concentrated within the saccular walls and beneath the endothelium of the pulmonary vasculature in a fibrilar pattern at P2 (Fig. 2G), and by P4 Postn expression intensified in the perivascular tissue and saccular walls, including the septal tips (Fig. 2H). Expression then

became restricted to the perivascular tissue again by P7 and P14 (Fig. 2I,J). Notably, the appearance of αSMA$^+$-myofibroblasts within the saccular walls coincided with the increase in Postn expression, as αSMA$^+$-cells were found only beneath large airways and large blood vessels at P0 (Fig. 2K). However, coincident with the expansion of Postn at P2, αSMA$^+$-myofibroblasts begin to appear within the saccular walls and capillaries (Fig. 2L), then localize to elongating septal tips at P4 and P7 (Fig. 2M,N). Then, when septal elongation is essentially complete by P14, αSMA-expressing cells are again absent from alveolar walls and are restricted to the large airways and pulmonary vasculature (Fig. 2O).

Immunoblotting of whole lung homogenates confirmed that peak Postn expression levels preceded maximal expression of αSMA protein (Fig. 2P,R). Compared with P0, Postn levels increased roughly threefold and twofold at P2 and P4, respectively, before rapidly declining to baseline P0 levels by P7, and then remained at low levels at P14 (Fig. 2Q). Multiple developmentally regulated differentially spliced isoforms of Postn are known to exist (Kruzynska-Frejtag et al., 2004; Snider et al., 2008), including secreted (90 kDa) and fibrilar forms (87 kDa and 85 kDa) (Fig. 2P, arrows). While the fibrilar isoforms were present in similar levels from birth through P14, secreted isoforms were prevalent at P2 and P4, suggesting that peak Postn expression was the result of a transient increase in secretion during saccular lung development and early alveolar septation. αSMA expression was relatively low at P0, but rapidly increased fivefold at P2, and peaked at nearly eightfold above P0 levels by P4 (Fig. 2R), correlating with when IHC (immunohistochemistry) revealed localization to the growing septal tips. Peak αSMA levels remained at P7 before significantly declining at P14 to levels similar to P0. Thus, peak Postn expression immediately precedes that of αSMA, but both proteins are transiently present and peak within the emergent septal tips during early alveolarization and both proteins are absent from alveolar walls immediately following normal rapid septal elongation. Additionally, these results demonstrate that Postn is both transcriptionally activated and translated within neonatal lungs themselves and is actively deposited within the remodeling lung interstitial cells during saccular morphogenesis.

Premature Downregulation of Postn Is a Marker for Interruption of an Important Early Window of Alveolar Development

The group led by O'Reilly has eloquently shown that brief hyperoxia exposure limited to just the first 4 days of murine lung development is sufficient to permanently simplify distal lung structure (Yee et al., 2009, 2011). Given the dramatic reduction of Postn we observed within two days of hyperoxia exposure, we used O'Reilly's model of targeted hyperoxia to determine if the downregulation of Postn occurred in a developmental window of lung injury capable of persistently inhibiting lung development. Following 85% O_2-exposure from P0 to P4, secondary septation was visibly stunted compared with room-air control littermates at P4 (Fig. 3A,C). Most significantly, P0 to P4 exposed mice recovered in room-air had persistently enlarged and simplified distal airspaces at P28 (Fig. 3B) as evidenced by a ~10% increase in MLI and ~10% decrease in nodal density (Fig. 3E,F; Table 1). Thus, despite recovery for over 3 weeks in room-air, there is incomplete alveolar septation following acute saccular lung injury. By gross inspection, septal tissue in hyperoxia-exposed mice at both P4 and P28 was thinned, suggestive of a lack of extracellular matrix (ECM) in

primary septa. Compared with controls, septal width was also significantly decreased by ~20% at P4 and P28 in hyperoxia-exposed animals (Table 1). Given this reduction in tissue density and lack of septal development that occurred following brief (P0–P4) hyperoxia exposure, we examined whether reduced proliferation or increased apoptosis might account for the morphological deficits observed in distal lung structure. Pups exposed to room-air demonstrated a steady increase in the percent of nuclei expressing the proliferative antigen, Ki67, within the saccular walls, from 12% at P2 to 24% at P4 (Fig. 3I–K). However, the percentage of proliferating cells in pups exposed to 85% hyperoxia was only 7% at P2 (Fig. 3G,K) and remained 9% at P4 (Fig. 3H,K) compared with room-air controls. Examination of the spatial distribution of the Ki67-positive cells revealed that they were mostly proliferating interstitial cells rather than the septal tip cells (Fig. 3I,J). To determine whether this detectable reduction of proliferating interstitial cells was due to elevated apoptosis or reduced proliferative rates, TUNEL analysis was performed. Significantly, apoptotic rates were extremely low in both P2 and P4 O_2-exposed and room-air controls (data not shown as less that 1 apoptotic cell/section detected). Thus, Postn downregulation occurs within a window of early lung injury associated with suppressed proliferation rates, diminished expression of α-SMA-myofibroblasts, thinned septal tissue, and blunted secondary septation that ultimately results in a persistent defect in alveolar complexity.

Postn Itself Is Not Required for the Appearance of Saccular Myofibroblast or Early Alveolar Morphogenesis

To determine whether the changes in the cell morphology and septal development require Postn, we examined the lungs from systemic *Postn*−/− mice (Rios et al., 2005) by morphology and immunohistochemical marker analysis. Using a different mutant line, it has been shown previously that alveolar development at P14 is normal in Postn knockout mice (Bozyk et al., 2012). However, neither accumulation of myofibroblasts in the saccular lung or early alveolar septation was examined. Given that we observed significant downregulation of Postn during a window of lung injury associated with diminished αSMA protein expression and persistent alveolar simplification, we sought to determine if loss of *Postn* inhibits normal myofibroblast accumulation or delays early septation. As anticipated, distal lung structure at both P4 (Fig. 4A,D,G,H) and P7 (Fig. 4B,E,G,H) was not significantly different between *Postn* nulls and controls, and lung development remained similar at 4 weeks of age (Fig. 4C,F–H). Morphometric data confirmed the histological appearance of absent early stage phenotype (Table 2). Likewise, the genetic absence of *Postn* throughout in utero development and during postnatal morphogenesis had no effect on the septal tip localization or levels of αSMA in the saccular lung (Fig. 4I–K), despite the fact that we observed a significant reduction and mis-localization of both proteins induced by means of hyperoxia at the P2 and P4 time-points. Thus, although a reduction of Postn is a useful marker of early lung injury and the presence of alveolar myofibroblasts, in the genetic absence of *Postn*, distal lung development is able to proceed grossly normally and αSMA expression and localization appears unaffected.

Absence of Postn Does Not Modulate the Inhibitory Effects of Acute Hyperoxia on Early Alveolar Septation

As it has previously been shown that the absence of Postn is sufficient to preserve alveolar development following chronic hyperoxia (Bozyk et al., 2012), and to extend and confirm the initial *Postn* knockout data above and test whether Postn may play a critical role during early acute hyperoxia-induced pathology, we subjected *Postn*−/− to various hyperoxia concentrations. To test whether the *Postn* nulls would be more sensitive to reduced hyperoxia, we initially exposed wild-type and *Postn*−/− mice to 60% O_2 from P0 to P7 and examined lung morphology. We failed to detect any statistically significant differences in septal phenotype between wild-type and *Postn* nulls exposed to 60% O_2 when compared with room-air (not shown). Given that acute 85% hyperoxia significantly downregulated Postn (Fig. 1), we next examined alveolar development in *Postn*−/− mice exposed to 85% hyperoxia to determine if the absence of Postn protected alveolar septation during this important early window of lung injury. Following 7 days of 85% hyperoxia, alveolar simplification was equally evident in both *Postn* knockout and wild-type mice (Fig. 5A–E), as evidenced by an increase in MLI of 18.4% and 16.4% and decrease in nodal density of 31.8% and 31.6% in knockouts and wild-types, respectively, compared with room-air exposed animals (Table 3). Thus, the genetic absence of *Postn* neither augments nor attenuates the inhibitory effects of hyperoxia on early alveolar septation.

DISCUSSION

Here we demonstrated that Postn expression is tightly correlated with the appearance of αSMA$^+$-myofibroblasts that are required for early alveolar septation in the developing murine lung. Additionally, in response to hyper-oxia, Postn responsiveness mirrors that of αSMA; as it is first downregulated by early exposure but then upregulated with continued, prolonged 85% O_2 exposure. However, Postn is not required for the localization or quantity of αSMA during normal distal lung morphogenesis, it is not required for normal alveolar septation, and the absence of *Postn* is not sufficient to exacerbate or attenuate the early inhibitory effect of hyperoxia on initiation of alveolar septation. These findings support the conclusion that, rather than directing their differentiation, Postn itself is more likely a useful marker of activated αSMA+-myofibroblasts and this would explain the tight association of Postn and αSMA-expression during both acute and chronic hyperoxia exposure. Thus, we conclude that mis-expression of Postn is an important bio-marker in the early and late phases of hyperoxia-induced murine neonatal lung pathology. Importantly, Postn may represent an additional molecular marker of the key myofibroblast lineage during early alveolar septation.

Preterm infants at greatest risk of developing BPD are born during early saccular lung development and early, acute lung injury predicts their likelihood of progression to BPD (Laughon et al., 2009, 2011). Similarly, hyperoxia exposure limited to murine saccular lung development is sufficient to interfere with early alveolar septation and permanently simplify adult alveolar structure and lung function (Yee et al., 2009, 2011; Yang et al., 2011). Although the multifactorial mechanisms are not well-defined, these observations support the conclusion that elevated O_2 levels are themselves teratogenic to the saccular and early

alveolar lung and are capable of interfering with ultimate alveolar complexity, surface area for gas exchange, and lung function. Despite a more sophisticated, lung-sparing strategy of neonatal care, as more extremely preterm infants survive, the incidence of BPD has not changed significantly (Fanaroff et al., 2007; Stoll et al., 2010). Multi-centered trials have suggested that early intervention improves survival without BPD more effectively that delayed therapies (Yost and Soll, 2000; Ballard et al., 2006). Unfortunately, the ability to predict which infants ultimately will develop BPD is inadequate based on prematurity alone. Cellular and protein bio-markers of significant, early lung injury are, therefore, being investigated as a means to improve predictive ability and maximize the efficacy and safety profile of preventative therapies (Bose et al., 2008; Baker et al., 2012; Schneibel et al., 2013). Although Postn can identify the development of fibrotic lung disease following prolonged injury, our study was designed to determine if Postn could similarly serve as a biomarker for early, significant lung injury. Within the developmental window immediately preceding early airspace simplification, we detected an acute downregulation of αSMA expression (a surrogate intracellular marker of saccular myofibroblasts) (Yamada et al., 2005) that correlated with a significant reduction of Postn. Because both downregulation of αSMA and Postn are tightly associated during acute hyperoxia, we conclude that the initial downregulation of Postn is a very early and useful robust biomarker of blunted myofibroblast accumulation and early alveolar septation.

Postn itself is not thought to provide a direct structural role but rather supports ECM organization/reorganization and cell behaviors including migration (Gillan et al., 2002), differentiation (Snider et al., 2008; Norris et al., 2009), collagen fibrillogenesis (Norris et al., 2007), and angiogenesis (Hakuno et al., 2010) during organogenesis and various reparative responses. In a pattern typical of matricellular proteins (Bornstein and Sage, 2002; Schroeder et al., 2003), we demonstrated that Postn was widely expressed in the saccular lung before being quickly restricted to the perivascular tissue during the alveolar stage. Peak Postn expression resulted from an increase in the secretory isoform during saccular lung development which coincided with expansion of myofibroblasts. Intriguingly, Postn expression directly correlated with the reduction in αSMA expression observed with acute hyperoxia as well as the increase in αSMA expression we et al. (Bozyk et al., 2012) have observed with chronic hyperoxia. Thus, we speculate that levels of Postn expression can serve as useful marker of both early physiologic (i.e., is suppressed) and late pathologic (i.e., is elevated) myofibroblastic differentiation. More importantly, because we determined that the secreted isoform of Postn is the predominate isoform affected by hyperoxia early on, we have identified a soluble marker of myofibroblast activity that potentially can be measured in tracheal aspirates of infants developing BPD. As αSMA is purely intracellular and cannot be measured in secretions, Postn may prove to be useful as a novel surrogate marker to follow myofibroblast activity during alveolar septal development and fibrotic lung injury.

Given Postn's robust expression within the neonatal lung and tight correlation with αSMA-expansion during early alveolar septation, as well as the significant reduction caused by hyperoxia within a window of lung injury capable of persistently inhibiting alveolar septation, we anticipated that the genetic absence of *Postn* could be sufficient to cause simplification of the early alveolar lung. However, examination of early alveolar

development in *Postn* knockout mice failed to reveal any significant differences from controls. These findings support the conclusion that, rather than directing the normal differentiation of myofibroblasts, Postn itself is a marker of αSMA^{+}-myofibroblasts. Thus, during acute hyperoxia exposure to the saccular lung, we speculate that hyperoxia disrupts the differentiation of αSMA-myofibroblasts, which are the predominant source of Postn (Bozyk et al., 2012), by means of a Postn-independent mechanism. Alternatively, the loss of *Postn* may result in the upregulation of other ECM proteins with similar function, especially in the context of our model of systemic deficiency. Indeed, Postn is one of four members of the fasciclin proteins expressed within the neonatal lung (data not shown) which each share a high degree of homology (Lindsley et al., 2005). βigH3, a protein that shares structural homology with Postn, was shown to be expressed within the alveolar septal tips of children but its significance is unknown (Billings et al., 2000); thus, compound mutants studies may be required to address potential genetic redundancy. Additionally, Postn is just one of an expanding list of matricellular proteins (Bornstein and Sage, 2002) known to be co-expressed within the developing lung, and other matricellular proteins including Tenascin-C (Kaarteenaho-Wiik et al., 2001), Galectin-1 (Foster et al., 2006), and Connective tissue growth factor (Burgos et al., 2010) may play a compensatory role or could act within a paralleled pathway capable of supporting lung morphogenesis in the absence of Postn. Further studies are needed to determine the significance of any possible compensatory and/or parallel mechanisms.

Postn nulls were not protected from the significant inhibition of early alveolar septation resulting from acute hyperoxia, further solidifying Postn's role as a marker rather than a primary effector of early hyperoxic lung injury. Thus, we conclude that the dramatic downregulation of Postn during acute hyperoxia exposure is not a compensatory, protective mechanism. Although these data may appear different from those of Bozyk et al. which examined the role of *Postn* in chronically inhibited alveolar septation (Bozyk et al., 2012), we suggest that the combined data reveal that Postn is a pleiotropic matricellular protein. In their report, Bozyk et al. demonstrated that an absence of *Postn* attenuated ectopic αSMA expression associated with fibrosis and preserved alveolar development following chronic hyperoxia at P14. However, there are several important differences in the model we used that may account for these dissimilarities. Our model used a higher percentage of hyperoxia (85% vs. 75%). Although this difference may appear insignificant, dose-dependent inhibition of alveolar development has been described (Yee et al., 2009). Indeed, we did not observe inhibition of either *Postn* null or wild-type animals exposed to 60% hyperoxia from P0 to P7, suggesting a threshold effect occurs between 60 and 85% hyperoxia. We also initiated hyperoxia at birth to encompass the critical saccular stage of lung development, while Bozyk et al. delayed hyperoxia until P2 to P3 when saccular development is nearly complete. The delay and/or resultant decrease in total hyperoxia exposure may have resulted in a more modest injury in their model. In agreement with Bozyk et al. we too found that Postn and αSMA were elevated at P14 following hyperoxia exposure (Fig. 1). Thus, we speculate that our results are representative of the early disease process and are distinct from the later secondary reparative response to severe lung injury that results in the eventual upregulation of Postn as a mediator of fibrosis consistent with other fibrotic pulmonary diseases (Takayama et al., 2006; Sidhu et al., 2010; Okamoto et al., 2011). Indeed, there is a

growing body of evidence linking the role of elevated Postn with pathological fibrosis in asthma (Woodruff et al., 2007; Gordon et al., 2012) and idiopathic pulmonary fibrosis (Okamoto et al., 2011).

Although Postn is mainly linked with pathological upregulation, our study highlights downregulation of soluble Postn as an early indicator of neonatal lung injury and identifies a potentially clinically useful biomarker of alveolar myofibroblasts and early inhibition of alveolar septation. Our findings also complement the previously reported association of subsequent upregulated Postn with excessive, prolonged myofibroblast activity during emerging fibrotic lung disease. Clinically correlating reduced Postn levels in tracheal aspirate fluid during windows of early BPD pathogenesis will be important to determine if Postn can serve as a useful, novel biomarker in preterm infants at risk for developing BPD and direct preventative therapies. Likewise, upregulation of Postn in tracheal aspirates from infants with progressive lung injury may provide a useful marker for interventional therapies to prevent fibroproliferation and promote normal lung development.

Acknowledgments

Supported by, in part, by KL2 RR025760 (S.K.A.; A. Shekhar, PI); as well as Riley Children's Foundation, the Indiana University Department of Pediatrics (Neonatal-Perinatal Medicine) and National Institutes of Health HL115619 (S.J.C.).

REFERENCES

Ahlfeld SK, Conway SJ. Aberrant signaling pathways of the lung mesenchyme and their contributions to the pathogenesis of broncho-pulmonary dysplasia. Birth Defects Res A Clin Mol Teratol. 2012; 94:3–15. [PubMed: 22125178]

Baker CD, Balasubramaniam V, Mourani PM, et al. Cord blood angiogenic progenitor cells are decreased in bronchopulmonary dysplasia. Eur Respir J. 2012; 40:1516–1522. [PubMed: 22496315]

Balasubramaniam V, Maxey AM, Morgan DB, et al. Inhaled NO restores lung structure in eNOS-deficient mice recovering from neonatal hypoxia. Am J Physiol Lung Cell Mol Physiol. 2006; 291:L119–L127. [PubMed: 16443642]

Balinotti JE, Chakr VC, Tiller C, et al. Growth of lung parenchyma in infants and toddlers with chronic lung disease of infancy. Am J Respir Crit Care Med. 2010; 181:1093–1097. [PubMed: 20133928]

Ballard RA, Truog WE, Cnaan A, et al. Inhaled nitric oxide in preterm infants undergoing mechanical ventilation. N Engl J Med. 2006; 355:343–353. [PubMed: 16870913]

Baraldi E, Carraro S, Filippone M. Bronchopulmonary dysplasia: definitions and long-term respiratory outcome. Early Hum Dev. 2009; 85(Suppl):S1–S3. [PubMed: 19793629]

Billings PC, Herrick DJ, Howard PS, et al. Expression of betaig-h3 by human bronchial smooth muscle cells: localization to the extracellular matrix and nucleus. Am J Respir Cell Mol Biol. 2000; 22:352–359. [PubMed: 10696072]

Bornstein P, Sage EH. Matricellular proteins: extracellular modulators of cell function. Curr Opin Cell Biol. 2002; 14:608–616. [PubMed: 12231357]

Bose CL, Dammann CE, Laughon MM. Bronchopulmonary dysplasia and inflammatory biomarkers in the premature neonate. Arch Dis Child Fetal Neonatal Ed. 2008; 93:F455–F461. [PubMed: 18676410]

Boström H, Gritli-Linde A, Betsholtz C. PDGF-a/PDGF alpha-receptor signaling is required for lung growth and the formation of alveoli but not for early lung branching morphogenesis. Dev Dyn. 2002; 223:155–162. [PubMed: 11803579]

Bozyk PD, Bentley JK, Popova AP, et al. Neonatal periostin knockout mice are protected from hyperoxia-induced alveolar simplication. PloS one. 2012; 7:e31336. [PubMed: 22363622]

Burgos CM, Nord M, Roos A, et al. Connective tissue growth factor expression pattern in lung development. Exp Lung Res. 2010; 36:441–450. [PubMed: 20939759]

Burri PH. Structural aspects of postnatal lung development - alveolar formation and growth. Biol Neonate. 2006; 89:313–322. [PubMed: 16770071]

Butcher JT, Norris RA, Hoffman S, et al. Periostin promotes atrioventricular mesenchyme matrix invasion and remodeling mediated by integrin signaling through Rho/PI 3-kinase. Dev Biol. 2007; 302:256–266. [PubMed: 17070513]

Coalson JJ. Pathology of bronchopulmonary dysplasia. Semin Perinatol. 2006; 30:179–184. [PubMed: 16860157]

Conway SJ. In situ hybridization of cells and tissue sections. Methods Mol Med. 1996; 6:193–206. [PubMed: 21380707]

Elliott CG, Wang J, Guo X, et al. Periostin modulates myofibroblast differentiation during full-thickness cutaneous wound repair. J Cell Sci. 2012; 125(Pt 1):121–132. [PubMed: 22266908]

Fanaroff AA, Stoll BJ, Wright LL, et al. Trends in neonatal morbidity and mortality for very low birthweight infants. Am J Obstet Gynecol. 2007; 196:147, e141–e148. [PubMed: 17306659]

Fawke J, Lum S, Kirkby J, et al. Lung function and respiratory symptoms at 11 years in children born extremely preterm: the EPI-Cure study. Am J Respir Crit Care Med. 2010; 182:237–245. [PubMed: 20378729]

Foster JJ, Goss KL, George CL, et al. Galectin-1 in secondary alveolar septae of neonatal mouse lung. Am J Physiol Lung Cell Mol Physiol. 2006; 291:L1142–L1149. [PubMed: 16891398]

Gillan L, Matei D, Fishman DA, et al. Periostin secreted by epithelial ovarian carcinoma is a ligand for alpha(v)beta(3) and alpha(v)beta(5) integrins and promotes cell motility. Cancer Res. 2002; 62:5358–5364. [PubMed: 12235007]

Gordon ED, Sidhu SS, Wang ZE, et al. A protective role for periostin and TGF-beta in IgE-mediated allergy and airway hyperresponsiveness. Clin Exp Allergy. 2012; 42:144–155. [PubMed: 22093101]

Hakuno D, Kimura N, Yoshioka M, et al. Periostin advances atherosclerotic and rheumatic cardiac valve degeneration by inducing angiogenesis and MMP production in humans and rodents. J Clin Invest. 2010; 120:2292–2306. [PubMed: 20551517]

Hirakawa H, Pierce RA, Bingol-Karakoc G, et al. Cathepsin S deficiency confers protection from neonatal hyperoxia-induced lung injury. Am J Respir Crit Care Med. 2007; 176:778–785. [PubMed: 17673697]

Husain AN, Siddiqui NH, Stocker JT. Pathology of arrested acinar development in postsurfactant bronchopulmonary dysplasia. Hum Pathol. 1998; 29:710–717. [PubMed: 9670828]

Jackson-Boeters L, Wen W, Hamilton DW. Periostin localizes to cells in normal skin, but is associated with the extracellular matrix during wound repair. J Cell Commun Signal. 2009; 3:125–133. [PubMed: 19543815]

Jiang JS, Lang YD, Chou HC, et al. Activation of the renin-angiotensin system in hyperoxia-induced lung fibrosis in neonatal rats. Neonatology. 2012; 101:47–54. [PubMed: 21791939]

Kaarteenaho-Wiik R, Kinnula V, Herva R, et al. Distribution and mRNA expression of tenascin-C in developing human lung. Am J Respir Cell Mol Biol. 2001; 25:341–346. [PubMed: 11588012]

Kim CJ, Yoshioka N, Tambe Y, et al. Periostin is down-regulated in high grade human bladder cancers and suppresses in vitro cell invasiveness and in vivo metastasis of cancer cells. Int J Cancer. 2005; 117:51–58. [PubMed: 15880581]

Kimura J, Deutsch GH. Key mechanisms of early lung development. Pediatr Dev Pathol. 2007; 10:335–347. [PubMed: 17929994]

Kruzynska-Frejtag A, Wang J, Maeda M, et al. Periostin is expressed within the developing teeth at the sites of epithelial-mesenchymal interaction. Dev Dyn. 2004; 229:857–868. [PubMed: 15042709]

Lau M, Masood A, Yi M, et al. Long-term failure of alveologenesis after an early short-term exposure to a PDGF-receptor antagonist. Am J Physiol Lung Cell Mol Physiol. 2011; 300:L534–L547. [PubMed: 21239531]

Laughon M, Allred EN, Bose C, et al. Patterns of respiratory disease during the first 2 postnatal weeks in extremely premature infants. Pediatrics. 2009; 123:1124–1131. [PubMed: 19336371]

Laughon M, Bose C, Allred EN, et al. Antecedents of chronic lung disease following three patterns of early respiratory disease in preterm infants. Arch Dis Child Fetal Neonatal Ed. 2011; 96:F114–F120. [PubMed: 20688867]

Lindahl P, Karlsson L, Hellstrom M, et al. Alveogenesis failure in PDGF-A-deficient mice is coupled to lack of distal spreading of alveolar smooth muscle cell progenitors during lung development. Development. 1997; 124:3943–3953. [PubMed: 9374392]

Lindsley A, Li W, Wang J, et al. Comparison of the four mouse fasciclin-containing genes expression patterns during valvuloseptal morphogenesis. Gene Expr Patterns. 2005; 5:593–600. [PubMed: 15907457]

Mitchell JJ, Reynolds SE, Leslie KO, et al. Smooth muscle cell markers in developing rat lung. Am J Respir Cell Mol Biol. 1990; 3:515–523. [PubMed: 2252578]

Morrisey EE, Hogan BLM. Preparing for the first breath: genetic and cellular mechanisms in lung development. Dev Cell. 2009; 18:8–23. [PubMed: 20152174]

Norris RA, Damon B, Mironov V, et al. Periostin regulates collagen fibrillogenesis and the biomechanical properties of connective tissues. J Cell Biochem. 2007; 101:695–711. [PubMed: 17226767]

Norris RA, Potts JD, Yost MJ, et al. Periostin promotes a fibroblastic lineage pathway in atrioventricular valve progenitor cells. Dev Dyn. 2009; 238:1052–1063. [PubMed: 19334280]

Okamoto M, Hoshino T, Kitasato Y, et al. Periostin, a matrix protein, is a novel biomarker for idiopathic interstitial pneumonias. Eur Respir J. 2011; 37:1119–1127. [PubMed: 21177844]

Rios H, Koushik SV, Wang H, et al. Periostin null mice exhibit dwarfism, incisor enamel defects, and an early-onset periodontal disease-like phenotype. Mol Cell Biol. 2005; 25:11131–11144. [PubMed: 16314533]

Roth-Kleiner M, Hirsch E, Schittny JC. Fetal lungs of tenascin-C-deficient mice grow well, but branch poorly in organ culture. Am J Respir Cell Mol Biol. 2004; 30:360–366. [PubMed: 12904321]

Ruan K, Bao S, Ouyang G. The multifaceted role of periostin in tumorigenesis. Cell Mol Life Sci. 2009; 66:2219–2230. [PubMed: 19308325]

Schneibel KR, Fitzpatrick AM, Ping XD, et al. Inflammatory mediator patterns in tracheal aspirate and their association with bronchopulmonary dysplasia in very low birth weight neonates. J Perinatol. 2013; 33:383–387. [PubMed: 23047424]

Schroeder JA, Jackson LF, Lee DC, Camenisch TD. Form and function of developing heart valves: coordination by extracellular matrix and growth factor signaling. J Mol Med (Berl). 2003; 81:392–403. [PubMed: 12827270]

Shimazaki M, Nakamura K, Kii I, et al. Periostin is essential for cardiac healing after acute myocardial infarction. J Exp Med. 2008; 205:295–303. [PubMed: 18208976]

Sidhu SS, Yuan S, Innes AL, et al. Roles of epithelial cell-derived periostin in TGF-beta activation, collagen production, and collagen gel elasticity in asthma. Proc Natl Acad Sci U S A. 2010; 107:14170–14175. [PubMed: 20660732]

Snider P, Hinton RB, Moreno-Rodriguez RA, et al. Periostin is required for maturation and extracellular matrix stabilization of noncardiomyocyte lineages of the heart. Circ Res. 2008; 102:752–760. [PubMed: 18296617]

Stoll BJ, Hansen NI, Bell EF, et al. Neonatal outcomes of extremely preterm infants from the NICHD neonatal research network. Pediatrics. 2010; 126:443–456. [PubMed: 20732945]

Takayama G, Arima K, Kanaji T, et al. Periostin: a novel component of subepithelial fibrosis of bronchial asthma downstream of IL-4 and IL-13 signals. J Allergy Clin Immunol. 2006; 118:98–104. [PubMed: 16815144]

Uchida M, Shiraishi H, Ohta S, et al. Periostin, a matricellular protein, plays a role in the induction of chemokines in pulmonary fibrosis. Am J Respir Cell Mol Biol. 2012; 46:677–686. [PubMed: 22246863]

Van Marter LJ. Epidemiology of bronchopulmonary dysplasia. Semin Fetal Neonatal Med. 2009; 14:358–366. [PubMed: 19783238]

Vrijlandt EJ, Gerritsen J, Boezen HM, et al. Lung function and exercise capacity in young adults born prematurely. Am J Respir Crit Care Med. 2006; 173:890–896. [PubMed: 16456146]

Warner BB, Stuart LA, Papes RA, Wispe JR. Functional and pathological effects of prolonged hyperoxia in neonatal mice. Am J Physiol Lung Cell Mol Physiol. 1998; 275:L110–L117.

Woodruff PG, Boushey HA, Dolganov GM, et al. Genome-wide profiling identifies epithelial cell genes associated with asthma and with treatment response to corticosteroids. Proc Natl Acad Sci U S A. 2007; 104:15858–15863. [PubMed: 17898169]

Yamada M, Kurihara H, Kinoshita K, Sakai T. Temporal expression of alpha-smooth muscle actin and drebrin in septal interstitial cells during alveolar maturation. J Histochem Cytochem. 2005; 53:735–744. [PubMed: 15928322]

Yang G, Hinson MD, Bordner JE, et al. Silencing hyperoxia-induced C/EBPalpha in neonatal mice improves lung architecture via enhanced proliferation of alveolar epithelial cells. Am J Physiol Lung Cell Mol Physiol. 2011; 301:L187–L196. [PubMed: 21571903]

Yee M, Chess PR, McGrath-Morrow SA, et al. Neonatal oxygen adversely affects lung function in adult mice without altering surfactant composition or activity. Am J Physiol Lung Cell Mol Physiol. 2009; 297:L641–L649. [PubMed: 19617311]

Yee M, White RJ, Awad HA, et al. Neonatal hyperoxia causes pulmonary vascular disease and shortens life span in aging mice. Am J Pathol. 2011; 178:2601–2610. [PubMed: 21550015]

Yoshioka N, Fuji S, Shimakage M, et al. Suppression of anchorage-independent growth of human cancer cell lines by the TRIF52/periostin/OSF-2 gene. Exp Cell Res. 2002; 279:91–99. [PubMed: 12213217]

Yost CC, Soll RF. Early versus delayed selective surfactant treatment for neonatal respiratory distress syndrome. Cochrane Database Syst Rev. 2000; 2:CD001456. [PubMed: 10796266]

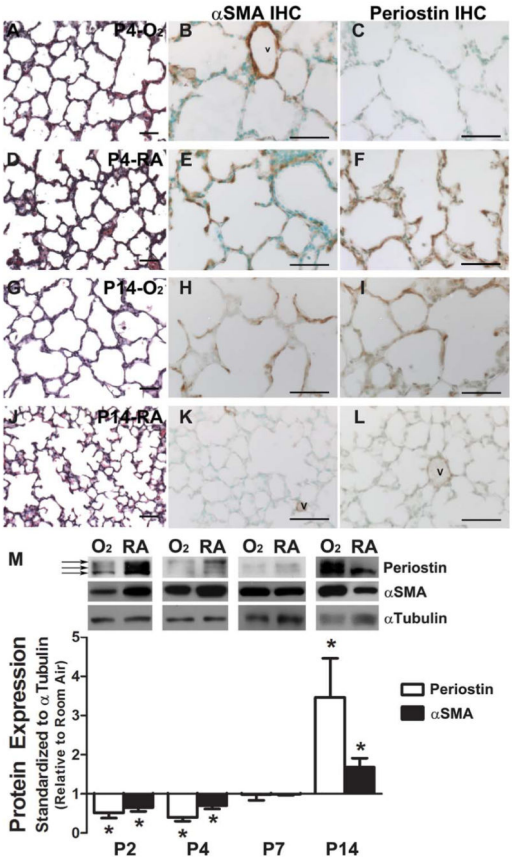

Figure 1.

Acute hyperoxia reduces expression of Periostin and αSMA protein in the saccular lung while chronic hyperoxia increases expression in the alveolar lung. Representative H/E and immunostaining for αSMA and Periostin in postnatal day 4 (P4) lungs continuously exposed to 85% hyperoxia (**A–C**) or room-air (**D–F**), as well as P14 lungs continuously exposed to hyperoxia (**G–I**) or room-air (**J–L**). (M) Representative immunoblots for Periostin and αSMA protein in whole lung homogenates from animals exposed to 85% hyperoxia (O_2) and room-air (RA) continuously from birth through P2, P4, P7, and P14. Arrows indicating 80 kDa and 84 kDa fibrilar (lower, middle arrows) and 90 kDa secreted (top arrow) isoforms of Periostin. Densitometry quantifying influence of continuous 85% hyperoxia exposure on whole lung protein levels of Periostin (white bars) and αSMA (black bars) compared with room-air at P2 to P14. N = 3 to 4 mice per group; Scale bars = 50 μm; *significant differences analyzed by Student's *t* test ($p < 0.05$ versus RA at equivalent postnatal ages); v, vessel.

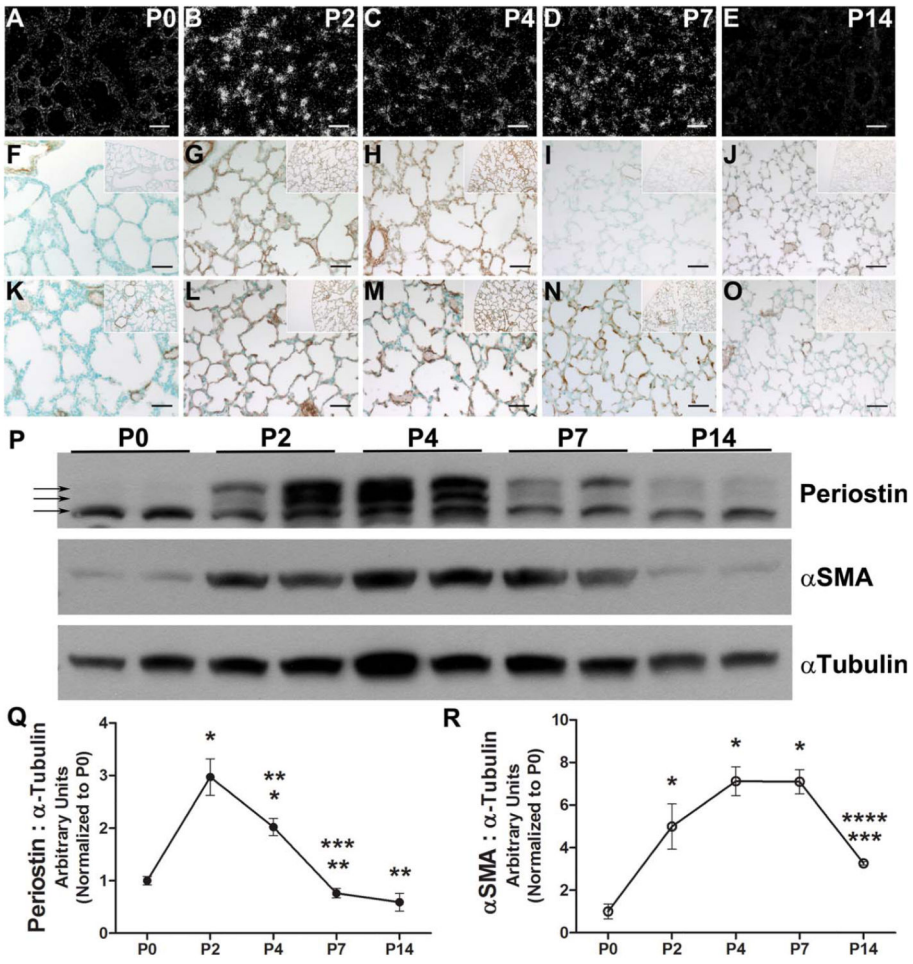

Figure 2.

Normal peak Periostin and αSMA expression occurs during postnatal saccular lung development. Representative photomicrographs of room-air exposed lungs at P0, P2, P4, P7, and P14 following in situ hybridization detection of Periostin mRNA (**A–E**), as well as immunostaining for Periostin (*F–J*) and αSMA (**K–O**) protein localization. Inserts represent lower-power images of pleural edge for orientation. **P:** Representative immunoblot quantification of Periostin and αSMA protein expression levels in duplicate whole lung homogenates from P0 through P14. Arrows indicating 80 kDa and 84 kDa fibrilar (lower, middle arrows) and 90 kDa secreted (top arrow) isoforms of Periostin. **Q,R:** Quantitative densitometry of immunoblots reveals Periostin levels (Q) peak before αSMA levels (R). N = 3 to 4 mice per group; Scale bars = 50 μm; significant differences analyzed by one-way analysis of variance with Tukey's multiple comparisons test ($p < 0.05$ vs. *P0, **P2, ***P4, and ****P7).

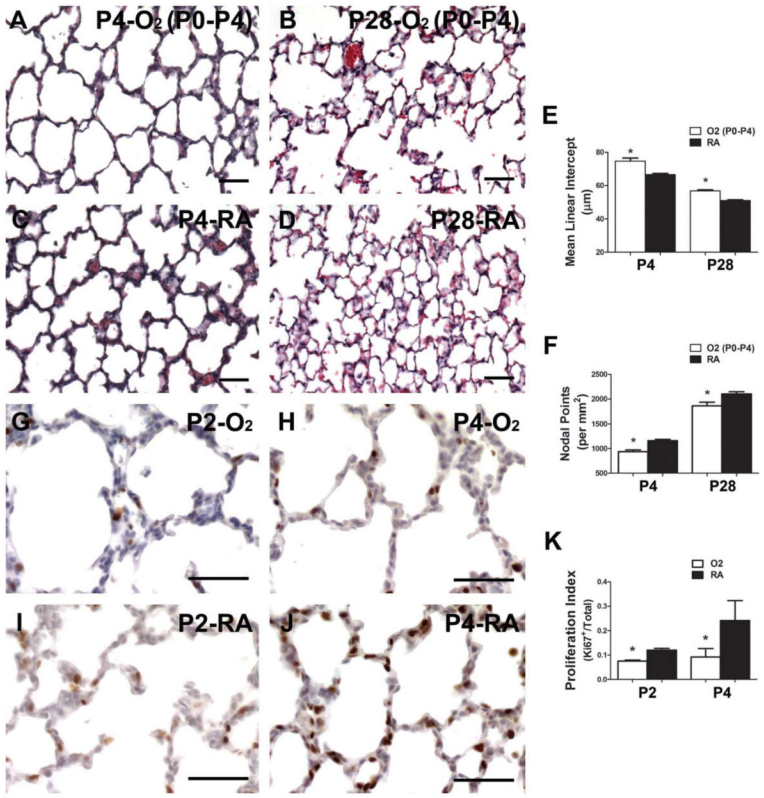

Figure 3.

Brief hyperoxia limited to saccular lung development inhibits distal lung cell proliferation and results in persistent defects in alveolarization. Representative H/E-stained lung sections from P4 animals transiently exposed to 85% hyperoxia (α) from P0 to P4, followed by recovery in room-air to P28 (**B**) compared with animals exposed to room-air continuously (**C,D**). **E,F**: Morphometric assessment of alveolar development by mean linear intercept (MLI) (E) and nodal density (F) at P4 and P28 in animals exposed to either transient 85% hyperoxia (white bars) or room-air (black bars) from P0 to P4 and then recovered in room-air until P28. G,J: Assessment of proliferation by means of immunostaining for Ki67 antigen at P2 (**G**) and P4 (**H**) in hyper-oxia and room-air (**I,J**) exposed lungs. **K**: Quantitative assessment of percentage of Ki67-positive cells in distal airspaces. N = 3 to 4 mice per group; Scale bars = 50 μm; *significant differences analyzed by Student's *t* test ($p < 0.05$ vs. RA at equivalent postnatal ages).

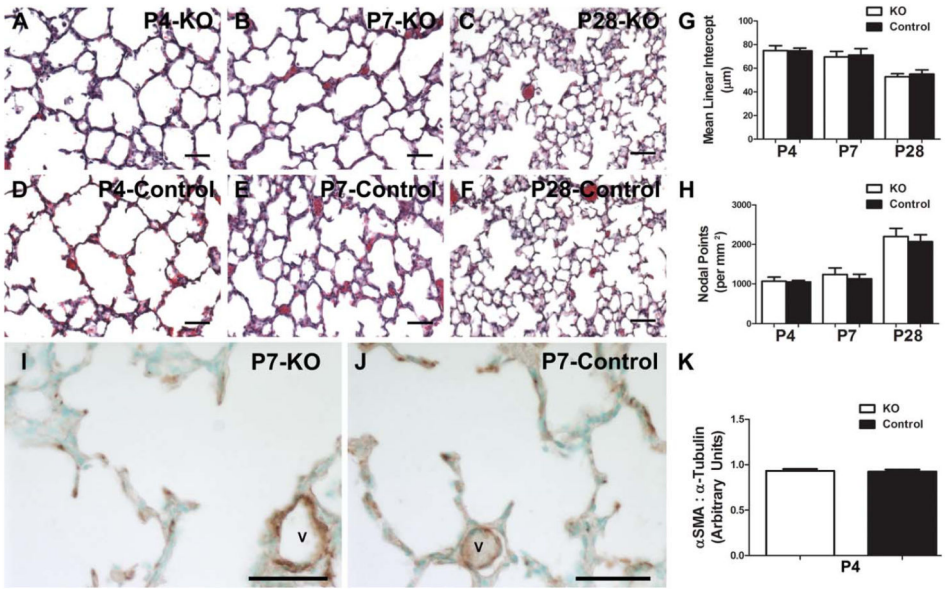

Figure 4.

Systemic loss of Periostin does not affect the presence of saccular lung myofibroblasts or ultimate alveolar development. Representative H/E stained lung sections from *Periostin* null (**A–C**) and age-matched littermate control (**D–F**) pups raised in room-air through P4, P7, and P28. **G,H**: Quantification of alveolar development by MLI (G) and nodal density (H). Immunostaining for αSMA in P4 *Periostin* null (**I**) and control (**J**) lungs. Note similar expression pattern within septal tips and around blood vessels (v). **K**: Whole lung αSMA levels at P4 were quantified by means of densitometry of immunoblots relative to α-Tubulin loading control. N = 3 to 7 mice per group; Scale bars = 50 μ; no significant differences when analyzed by Student's *t* test ($p > 0.05$ vs. control at equivalent postnatal ages).

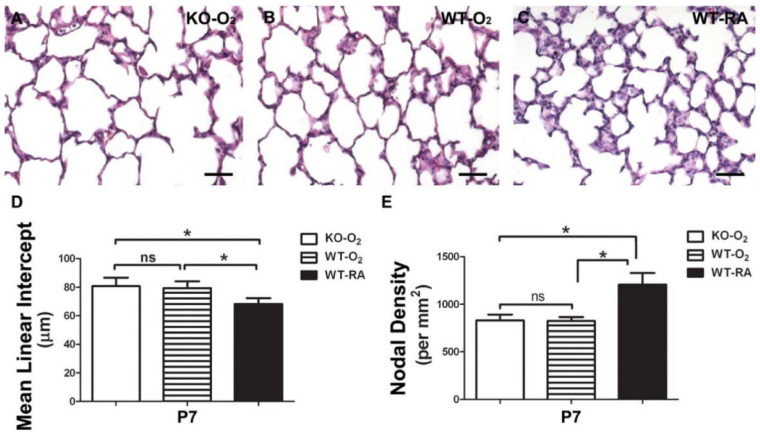

Figure 5.

Genetic absence of Periostin does not protect the early developing lung during acute hyperoxia exposure. Representative H/E stained P7 lung sections from *Periostin* null (**A**) and age-matched littermate wild-type pups (**B**) exposed to continuous 85% hyperoxia from P0 to P7 compared with wild-type mice raised in room-air (**C**). **D,E**: Quantification of alveolar development by MLI (D) and nodal density (E) revealed that both *Periostin* null and wild-type lungs were equally aberrantly affected by means of 85% O_2. N = 7 mice per group; Scale bars 5 50 μm; *significant differences analyzed by one-way analysis of variance with Tukey's multiple comparisons test ($p < 0.05$ vs. RA at equivalent postnatal ages); ns, nonsignificant ($p > 0.05$).

Table 1

Effects of Continuous Hyperoxia on Distal Lung Structure from Birth through to P14, as Well as Brief Hyperoxia from P0 to P4 followed by Recovery in Room Air through P28

Postnatal age-exposure (N)	MLI (μm)	Nodal density (points per mm^2)	Septal thickness (μm)
P4-O_2 (5)	74.66 ± 1.93[a]	937 ± 36[a]	11.34 ± 0.68[a]
P4-RA (4)	66.62 ± 0.65	1160 ± 27	14.07 ± 0.59
P7-O_2 (4)	83.22 ± 2.87[a]	847 ± 46[a]	12.35 ± 1.0[a]
P7-RA (4)	69.96 ± 1.74	1230 ± 95	19.54 ± 0.69
P14-O_2 (3)	92.70 ± 3.56[a]	680 ± 24[a]	9.67 ± 0.14[a]
P14-RA (4)	61.75 ± 1.57	1720 ± 118	16.21 ± 1.10
P28-O_2(P0–P4) (3)	56.82 ± 0.62[a]	1861 ± 74[a]	12.02 ± 0.96[a]
P28-RA (4)	51.01 ± 0.52	2103 ± 44.53	14.98 ± 0.35

Values are means ± SEM.

MLI, mean linear intercept; O_2, 85% hyperoxia; RA, room-air.

[a]Significant differences analyzed by Student–s t test ($p < 0.05$ vs. RA at equivalent postnatal ages).

Table 2

Normal Distal Lung Development in the Presence and Absence of Periostin

Postnatal age-genotype (N)	MLI (μm)	Nodal density (points per mm^2)
P4-Null (6)	74.99 ± 1.67	1066 ± 43
P4-Control (5)	74.72 ± 1.03	1048 ± 17
P7-Null (5)	69.57 ± 2.13	1240 ± 72
P7-Control (3)	71.09 ± 3.19	1128 ± 68
P28-Null (4)	52.76 ± 1.32	2202 ± 102
P28-Control (7)	55.05 ± 1.37	2070 ± 65

Values are means ± SEM. no significant differences when analyzed by Student's t test ($p > 0.05$ vs. control at equivalent postnatal ages).

MLI, mean linear intercept.

Table 3

Distal lung Development following Acute 85%-O_2 in the Absence and Presence of Periostin

Postnatal age-genotype-exposure (N)	MLI (μm)	Nodal density (points per mm^2)
P7-Null-O_2 (7)	80.77 ± 2.23[a]	829 ± 23[a]
P7-WT-O_2 (7)	79.38 ± 1.80[a]	825 ± 15[a]
P7-WT-RA (7)	68.20 ± 1.57	1206 ± 46

Values are means ± SEM.

MLI, mean linear intercept.

[a]Significant differences analyzed by one-way analysis of variance with Tukey's multiple comparisons test ($p < 0.05$ vs. WT-RA).